Modal Analysis of Delaminated Flax Fibre Reinforced Epoxy Composite Plate

*Zi Cong Ho, Choe Yung Teoh**
Faculty of Engineering and Technology,
Tunku Abdul Rahman University College, Kuala Lumpur, Malaysia
**teohcy@tarc.edu.my*

ABSTRACT

This paper describes the influence of fibre orientation, delamination size and location on the natural frequencies of the single mid-plane delaminated unidirectional flax fibre reinforced epoxy (FFRE) composite plates under different boundary conditions numerically by using ANSYS MAPDL. The delaminated composite plate was modelled as two separate volumes divided at the midplane of the plate, with the nodes on the intact surfaces merged. In contrast, the nodes on the delaminated region remained separate. The results show that the CCCC delaminated composite plate has the highest fundamental natural frequency (219.996 Hz). Furthermore, for increasing fibre orientation from 0° to 45°, the fundamental natural frequencies decreased by 10.12% for the CCCC condition and increased by 6.01% for the SSSS condition. The fundamental natural frequency for the cantilever condition decreased 60.91% when fibre orientation increased to 90°. Moreover, the CCCC condition significantly reduces the fundamental natural frequency (up to 38.95%) with increasing delamination size. For CCCC and SSSS conditions, the centre delamination possesses the highest fundamental natural frequency (219.996 Hz and 116.525 Hz, respectively). The highest fundamental natural frequency for cantilever conditions is 33.081 Hz, with delamination located at the middle of the width and near the free end.

Keywords: *Delamination; Natural Fibre Composite Plate; Natural Frequency; Finite Element Analysis*

ISSN 1823-5514, eISSN 2550-164X

Received for review: 2022-04-22
Accepted for publication: 2022-07-17
Published: 2022-09-15

Introduction

Fibre-reinforced composite laminates have been used extensively in the aerospace, automotive, naval, civil, sports equipment, prosthetics, and even the arms industries. However, despite the advantages offered by fibre reinforced polymer (FRP) composites, they are still vulnerable to various defect modes like other materials. The defects of FRP composites are buckling, inclusions, matrix crack, broken fibres, and delamination [1]. Delamination is the most frequently found damage in composites that may be produced for different reasons among the mentioned defects. Delamination is a type of damage where the fibre plies separate from each other and tremendously reduce the structure's strength and stiffness.

Consequently, reducing stiffness also influences dynamic characteristics such as natural frequency and mode shape [2]. Therefore, even though the structure will not fail immediately, the delamination area may continue to grow and reduce its stiffness. As a result, the structure will eventually fail, although it is yet to meet the designed failure points. In recent decades, the effects of human activities on the environment have become noticeable and intensified. Subsequently, these had increased the environmental awareness of multiple countries, which led to the formation of many environmental policies and agreements, both intra- and internationally. Among the pool of solutions, green composites (natural fibres) have been trending in recent years, attracting the involvement of many researchers in researching and developing environmental-friendly materials across various industries to replace synthetic fibres.

Hu et al. [3] had proposed a C_0-type finite element method model, which is based on the simple higher-order theory to analyse the influence of delamination size on the reduction of the natural frequency of an 8-layer $[0°/90°]_{2s}$ square plate with all four edges in the clamped boundary condition. Shu and Della studied the free vibration of composite beam with single, double (same length), and two enveloping (one short and one long) delamination by using an analytical solution derived from the Euler – Bernoulli beam theory [4]. Mohanty et al. conducted numerical and experimental investigations on the natural frequency of delaminated woven glass/epoxy composite plates under five different manipulating parameters [5]. The parameters are delamination area, boundary conditions, fibre orientations, number of ply layers, and the aspect (width-over-length) ratio. Goren Kiral et al. [6] carried out vibration analysis of periodic axial loading on the delaminated glass/epoxy composite cantilever beams experimentally and numerically using Bolotin's approach in the commercial numeric computing software – MATLAB. The study also includes the change of natural frequency in delaminated woven glass/epoxy composite beam under the variations of delamination location and stacking sequences. Meon et al. [7] developed a three-dimensional progressive damage finite element model to detect delamination and examine the failure

modes and structural response of carbon fibre reinforced epoxy composite subjected to low-velocity impact loading. Hung et al. [8] conducted a free vibration analysis of laminated functionally graded carbon nanotube-reinforced composite (FG-CNTRC) plates with four different patterns of single-walled carbon nanotubes (SWCNTs) by using the pb2-Ritz method.

The application of natural FRP composite materials in transportation, civil and sports industries has raised the attention on studying FRP composites' vibration and damping behaviour. For instance, Daoud et al. [9] investigated the influence of ply orientation on the vibration properties of unidirectional Flax fibre-reinforced composite. Rajesh and Pitchaimani [10] examined experimentally and numerically the free vibration and buckling behaviours of different numbers of layers and types of the woven natural fibre-reinforced composite beam when compression load is applied to the axial direction. Mahmoudi et al. [11] conducted experimental and numerical investigations on the damping properties of flax fibre-reinforced epoxy plates by implementing a homogenization technique with a finite iso-parametric shell element. Recently, Gopalan et al. [12] reported the experimental and numerical investigation of the free vibration analysis of woven Flax/Bio-epoxy laminated composite plates with different stacking sequences, structural support and plate aspect ratio. Tharazi et al. [13] conducted a study to identify the optimum fibre content percentage for long unidirectional kenaf fibre reinforced polylactic-acid composites. Yunus et al. [14] evaluated the influence of low energy impact on the short kenaf fibre reinforced epoxy composites in terms of residual strength and stiffness. Ravandi et al. [15] examined tensile loading delamination propagation and internal fracture toughness in a stitched unidirectional flax fibre. They studied the untwisted flax yarn stitches and unstitched flax fibre-reinforced epoxy composites using double cantilever beam (DCB) testing. Another study of delaminated Flax fibre-reinforced epoxy composites was done by Shen et al. [16]. They investigate delamination detection by changing dynamic mechanical properties. Harun et al. [17] investigated the effects and determined the optimum range of the milling parameters to reduce the delamination factor (F_d) in milling operation to kenaf fibre reinforced polymer composite.

Based on the above literature review, there are numerous studies on the intact flax FRP composites but only a few on the delamination of flax FRP composites. Especially on the vibration analysis of delaminated composite. Therefore, this paper investigated the effect of stacking sequences, delamination size and location on the natural frequencies of the delaminated FFRE composite plates. The parametric study was conducted numerically using the commercial simulation software – Mechanical ANSYS Parametric Design Language (ANSYS MAPDL).

Methodology

Finite element modelling in ANSYS MAPDL

This project used the three-dimensional layered solid element SOLID185 to simulate both intact and delaminated FFRE composite plates. SOLID185 element has eight nodes with three translational degrees of freedom in the x, y, and z axes. Therefore, SOLID185 can create the composite model in three-dimension compared to the shell element in which the model was developed in two-dimension. Then, the layer information of the composite, such as the thickness of each ply and fibre orientation, was defined using the software's shell section function. Two different methods were used to model the intact and delaminated composite model. The intact composite was created as one complete volume model, while the delaminated composite was created as two separate volumes detached at the plane where delamination is located. To simulate the delamination effect, the nodes of the two volumes in the intact regions are merged while the nodes in the delaminated regions remain separate.

To simplify the identification of the delamination location along the X and Y axes, the delamination location is addressed by the normalised distances with respect to the length and width of the plate. Consider the distance from the centre of the delamination to the origin in the X-direction is termed as L while the distance to the origin in Y-direction is termed as W shown in Figure 1. The normalised distance in the X-direction will be labelled as l, which is the ratio of L to L_0 (plate length). The normalised distance in Y-direction will be labelled as w, which is the ratio of W to W_0 (plate width). To obtain a more realistic delamination simulation, contact pairs were implemented between the nodes of the delaminated regions by creating the contact elements (TARGE170/CONTA174) between the surfaces. The contact pair was implemented with the "Standard" contact behaviour in which the normal and tangent penalty stiffness of $1 \times 10^6 N/m$ will be set to prevent them from intersecting. Other than contact behaviour, the contact pair had zero friction coefficient to simulate complete separation between plies at the delaminated region in real life.

Research framework

Two sets of results obtained by other researchers will be the baseline for simulation validation of the intact and delaminated composites model. First, the intact laminated unidirectional FFRE composite beam was modelled, and modal analysis was conducted. The dimension of the intact FFRE composite cantilever beam and material properties are shown in Table 1. Two beams consisting of 8 layers of the unidirectional lamina, namely $[0°]_8$ and $[90°]_8$ were modelled and underwent modal analysis to obtain the first four natural frequencies for each fibre orientation. The results were compared with the

researched results by Daoud et al. [9] in Table 3, which showed good agreement between the present results and the researchers' results.

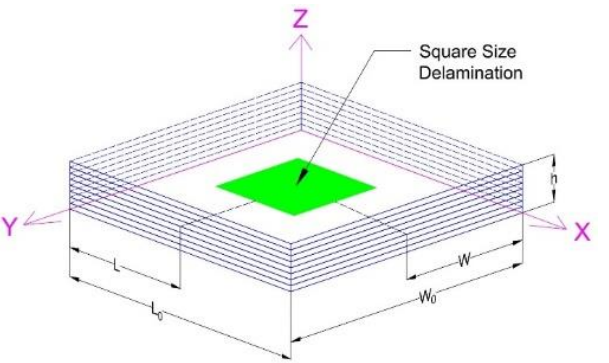

Figure 1: Schematic diagram of delaminated composite plate

After that, a 25% delaminated cross-ply carbon fibre reinforced polymer (CFRP) composite square plate with a stacking sequence of $[0°/90°]_{2S}$ will be modelled with its dimension and material properties shown in Table 2. The delamination size is half the length of the plate (0.0635 m) and is located at the centre between the middle layers. Then, the plate will undergo modal analysis to obtain the fundamental natural frequency. The results were compared with Hu et al. [3] in Table 4 to validate the delamination simulation setup. Excellent agreement was found between the present and the researchers' results with a low percentage error (0.49%).

Table 1: FFRE composite's material properties and beam's dimension [9]

Dimension of FFRE Composite Beam:	
Number of Layers	8
Length (*m*):	0.25
Width (*m*):	0.02
Thickness (*m*):	0.003
Material Properties for Each Layer:	
Longitudinal Young's Modulus, E_{11} (*GPa*):	22.2
Transverse Young's Modulus, E_{22} (*GPa*):	3.2
Shear Modulus, G_{12} (*GPa*):	1.33
Poisson's Ratio, *v*:	0.4
Density, ρ (kg/m^3):	1150

Table 2: Dimension and material properties of CFRP composite plate [3]

Dimension of CFRP Composite Plate:	
Stacking Sequence:	$[0°/90°]_{2S}$
Length (*m*):	0.127
Width (*m*):	0.127
Thickness (*m*):	0.001016
Material Properties for Each Layer:	
Longitudinal Young's Modulus, E_{11} (*GPa*):	134
Transverse Young's Modulus, E_{22} (*GPa*):	10.3
Shear Modulus (Longitudinal Plane), G_{12} (*GPa*):	5
Shear Modulus (Transverse Plane), G_{23} (*GPa*):	3.28
Poisson's Ratio, *v*:	0.33
Density, ρ (kg/m^3):	1480

Table 3: Results comparison of natural frequencies of cantilever FFRE composite plate

		Natural Frequency (*Hz*)			
Fibre Orientation		**0°**		**90°**	
		Daoud et al. [3]	Present	Daoud et al. [3]	Present
Mode	1	35	33.581	13	12.886
	2	210	210.120	86	80.797
	3	613	586.802	230	226.479
	4	1347	1145.430	465	444.581

Table 4: Results comparison of natural frequencies for delaminated four-side clamped CFRP composite plate.

Delamination Size	**Natural Frequency (*Hz*)**	
	Hu et al. [9]	Present
$(0.0635\ m)^2$	600	597.073

After the models were validated, the models were used to analyse the natural frequencies of the delaminated FFRE composite plates under different stacking sequences, delamination size, delamination location, and boundary conditions. The material properties of the FFRE composite plate were obtained from work done by Daoud et al. [9], as shown in Table 1, while the dimension of the square plate was set to be 0.25 m. The boundary conditions that will be considered are four-edge simply supported (SSSS), four-edge clamped (CCCC) and cantilever (CFFF). The stacking sequences that were studied in this project are $[0°]_8$, $[15°]_8$, $[30°]_8$, $[45°]_8$, $[60°]_8$, $[75°]_8$, and $[90°]_8$. The

delamination sizes considered are 0.0% (intact), 12.5%, 25%, 50%, and 75% square delamination located at the centre and between the middle plies. Furthermore, nine delamination locations were studied using normalised distances at 0.35, 0.5 and 0.65 in length and width, respectively. The modal analysis was set to obtain the first ten modes of vibration.

Results and Discussion

A mesh convergence test was conducted to obtain the mesh size used throughout the research to ensure the element size will not affect the results. The results were found to converge after 20000 elements. The corresponding mesh has 50 elements along the length and width, with one element representing one layer along with the thickness.

Effect of boundary conditions

The variation of boundary conditions against the natural frequencies was plotted in Figure 2. It is observed that the delaminated FFRE composite plate has the highest natural frequencies under CCCC conditions with the values of 219.996 Hz and 804.122 Hz for Mode 1 and Mode 10 respectively. The lowest natural frequencies occur when the delaminated plate is under CFFF conditions, with 32.709 Hz for Mode 1 and 424.262 Hz for Mode 10. This relation is similar to the glass fibre epoxy composite plates obtained by Mohanty et al. [5] and Ganesh et al. [18]. The fundamental natural frequency for SSSS and CFFF conditions reduce by 47.03% and 85.13%, respectively, compared to CCCC conditions. The figure shows that the boundary conditions greatly influence the natural frequency for all ten modes. The four sides clamped plate has greater natural frequencies than the others because the clamped edge will result in greater elastic rigidity and clamping effects than simply supported and free end edges.

Effect of Fibre Orientations

The delamination was fixed with the size of 25% located at the centre of the middle plies in this investigation. In addition, each stacking sequence was subjected to different boundary conditions to examine further the influence of fibre orientations under different boundary conditions.

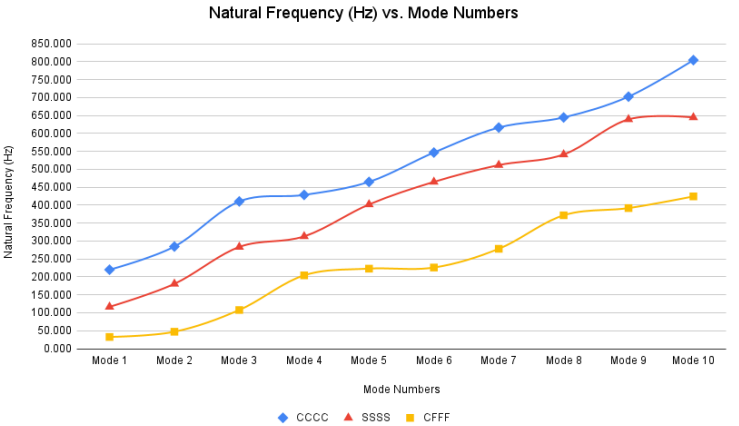

Figure 2: Graph of natural frequency against mode numbers for 25% delamination $[0°]_8$ FFRE composite plate under different boundary conditions

CCCC boundary condition

The first ten natural frequencies of each stacking sequence of 25% delamination FFRE composite plate with CCCC condition are shown in Figure 3. From Figure 3, it is noticed that the fundamental natural frequency decreased with increasing fibre orientation from 0° (219.996 *Hz*) to 45° (197.732 *Hz*). The fundamental natural frequency for $[15°]_8$, $[30°]_8$ and $[45°]_8$ decreased by 2.55%, 7.64% and 10.12%, respectively. The result indicates that the composite plate's flexural stiffness decreases when the ply's fibre orientation increases. Subsequently, the decrease in stiffness results in the natural frequency reduction as the fibre orientation increases. After 45°, similar to the results obtained by Samyal et al. [19], the natural frequency for 60° to 90° fibre orientation is the value for 0° to 30°, which is inverted horizontally with respect to the 45° fibre orientation. This inversion trend is also observed for other modes' frequencies. This is because the composite plate has symmetric boundary conditions on the x-axis and y-axis with equal length and width. From Figure 3, it is observed that the decreasing trend for fundamental natural frequency does not apply to other modes' frequencies; rather, the values fluctuate for different modes.

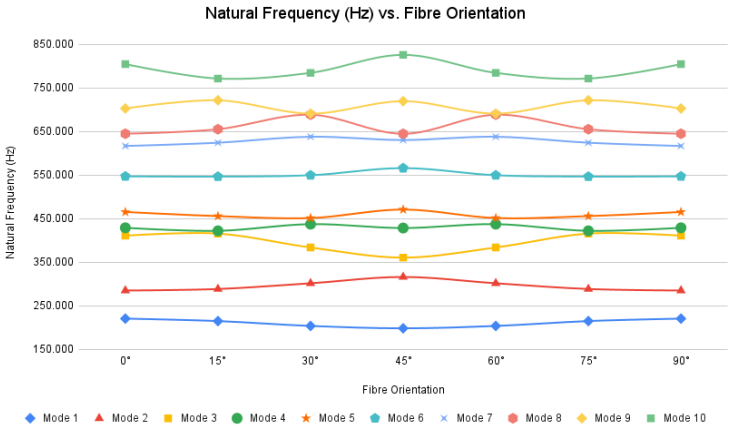

Figure 3: Graph of first ten natural frequency against fibre orientation for 25% delamination FFRE composite plate under CCCC boundary condition

SSSS boundary condition

The effects of fibre orientations on the first ten natural frequencies were plotted in Figure 4. Based on Figure 4, it is observed that the natural frequency increased as the fibre orientation increased from 0° (116.525 Hz) to 45° (123.531 Hz). The fundamental natural frequency for $[15°]_8$, $[30°]_8$ and $[45°]_8$ increased by 1.19%, 4.15% and 6.01%, respectively. In contrast with the CCCC condition, the SSSS condition causes the flexural stiffness of the composite plate to increase with increasing fibre orientation and thus increases the natural frequency. Similar to the CCCC condition, after 45°, the natural frequency for fibre orientation from 60° until 90° is the horizontal inverted value for 0° to 30° with respect to the 45° fibre orientation. An identical trend is also noticed for other modes' frequencies.

CFFF boundary condition

The influence in the first ten mode's frequencies as a function of fibre orientation is plotted in Figure 5. From Figure 5, it is observed that the fundamental natural frequency decreased with increasing fibre orientation, as described by Mohanty et al. [5], CFFF condition with the stacking sequence of [0°]8 compared to other unidirectional fibre orientations. This is because the 0° fibre plies are perpendicular to the clamped edge in which the bonding between fibres and polymer resists the deflection. However, for 90° fibre plies, the primary resistance to resist deflection is mainly provided by the polymer of the composite, which binds the fibre plies together. The trend from 0° to 45° is similar to the CCCC condition, whereby the frequency decreased rapidly and then decreased exponentially after 30°. The maximum fundamental

frequency (32.709 Hz) occurred at 0°, whereas the minimum frequency (12.786 Hz) was at 90°.

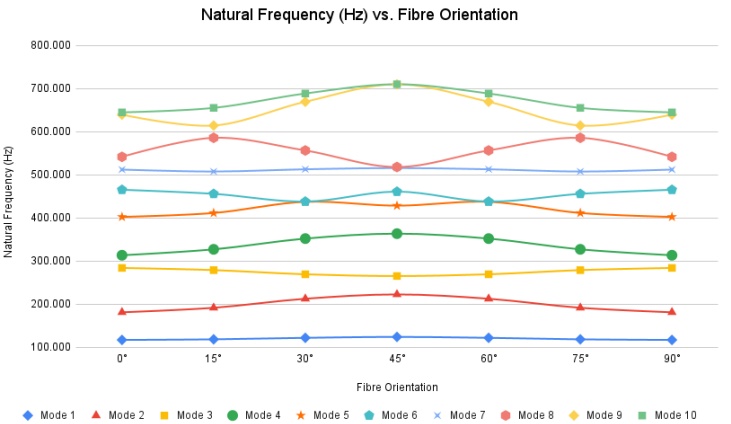

Figure 4: Graph of first ten natural frequency against fibre orientation for 25% delamination FFRE composite plate under SSSS boundary condition

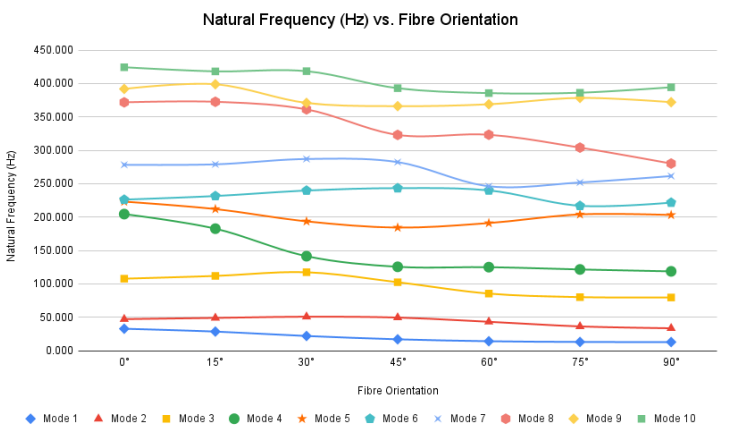

Figure 5: Graph of first ten natural frequency against fibre orientation for 25% delamination FFRE composite plate under CFFF boundary condition

Effect of delamination size

In this study, the delamination was introduced at the centre of the plate in between the middle plies. Five delamination sizes were investigated with different boundary conditions.

CCCC boundary condition

Table 5 shows the changes in natural frequencies of the composite plate with the five different delamination sizes under CCCC boundary conditions. The frequency variation as a function of delamination size was plotted as shown in Figure 6. Based on Figure 6, it is observed that the fundamental natural frequency decreased with increasing delamination size. In addition, it is found that the reduction is greater at a greater delamination size, which is similar to the findings of Hu et al. [3], and Mohanty et al. [5]. The phenomena are due to adhesive loss between the plies at the delaminated region. With a greater delamination area, less stress is required to deform the composite plate plastically and elastically. Thus, the elastic stiffness of the plate will reduce and cause the flexural stiffness and natural frequency to decrease. From Table 5, it is noticed that the natural frequency for all ten modes decreased when the delamination size increased. It is worth highlighting that the natural frequency for higher modes experienced a more significant reduction than for lower modes. The reduction of natural frequency for Mode 1 from 12.5% to 75.0% of delamination size with respect to the intact model are 0.94%, 6.63%, 23.79% and 38.95% respectively.

Table 5: Natural frequencies (Hz) for $[0°]_8$ FFRE composite plate under CCCC boundary condition with different delamination size

Mode	**Delamination Size**				
	0.0%	**12.5%**	**25.0%**	**50.0%**	**75.0%**
1	235.62	233.41	220.00	179.56	143.85
2	336.14	313.93	284.50	242.55	202.19
3	528.86	489.40	410.32	285.32	230.14
4	597.70	495.08	428.46	358.11	277.97
5	670.63	635.51	464.75	368.28	314.22
6	807.82	717.00	546.53	402.12	358.73
7	819.86	773.97	616.23	465.37	384.72
8	1058.73	901.20	644.34	507.82	402.61
9	1146.45	965.53	702.33	542.42	427.24
10	1167.90	987.27	804.12	576.49	471.21

SSSS boundary condition

The natural frequencies of the FFRE composite plate with different delamination sizes under SSSS boundary conditions were tabulated in Table 6. Figure 7 shows the effects of delamination sizes on the fundamental natural frequency under this boundary condition. From the figure, the fundamental natural frequency has the expected trend similar to the CCCC condition. The decrease in the natural frequency was also applied to the other modes, as observed in Table 6. Besides, a similar trend in the CCCC condition was spotted for the SSSS condition, where the natural frequency decreases more

rapidly at greater mode. However, the natural frequency reduction for the SSSS condition is less than the CCCC condition. The reduction of natural frequency for Mode 1 from 12.5% to 75.0% of delamination size with respect to the intact model are 0.17%, 1.35%, 7.11% and 15.96% respectively.

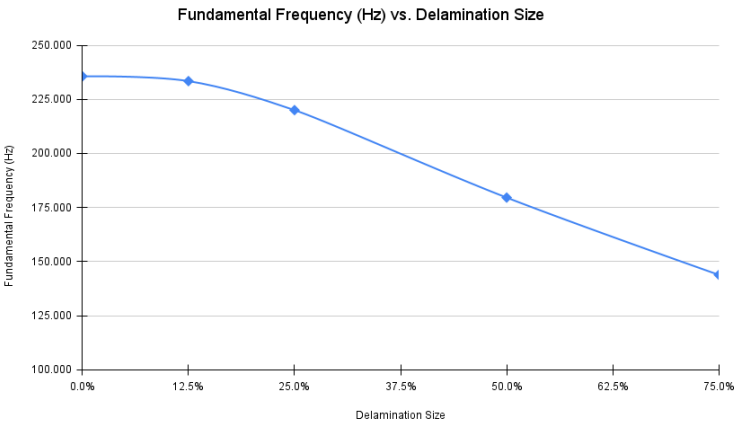

Figure 6: Graph of fundamental frequency against delamination size for $[0°]_8$ FFRE composite plate under CCCC boundary condition

Table 6: Natural frequencies (Hz) for $[0°]_8$ FFRE composite plate under SSSS boundary condition with different delamination size

Mode	Delamination Size				
	0.0%	**12.5%**	**25.0%**	**50.0%**	**75.0%**
1	118.12	117.92	116.52	109.73	99.27
2	209.77	198.95	180.61	157.45	141.84
3	385.34	348.35	283.48	233.78	217.20
4	403.94	367.83	312.90	255.01	230.14
5	471.38	456.94	401.88	285.32	234.39
6	612.31	575.23	464.74	321.09	277.97
7	640.34	579.90	511.57	368.28	280.86
8	838.95	795.53	541.12	399.72	354.42
9	882.21	801.01	639.05	443.39	378.09
10	940.57	836.78	644.34	520.60	384.71

CFFF boundary condition

Table 7 7 shows the natural frequency of the composite plate with different delamination sizes under CFFF conditions. Figure 8 shows the changes in the fundamental natural frequencies on different delamination sizes under this boundary condition. Based on the figure, the fundamental natural frequency

for the CFFF condition has a matching trend to the other two boundary conditions where the natural frequency decreased with increasing delamination size. The reduction in natural frequency for the CFFF condition is slightly greater than for the SSSS condition. The natural frequency for Mode 1 from 12.5% to 75.0% of delamination size with respect to the intact model decrease by 0.72%, 2.84%, 9.24% and 17.49% respectively. Nevertheless, after Mode 1, the reduction is less significant than the SSSS condition.

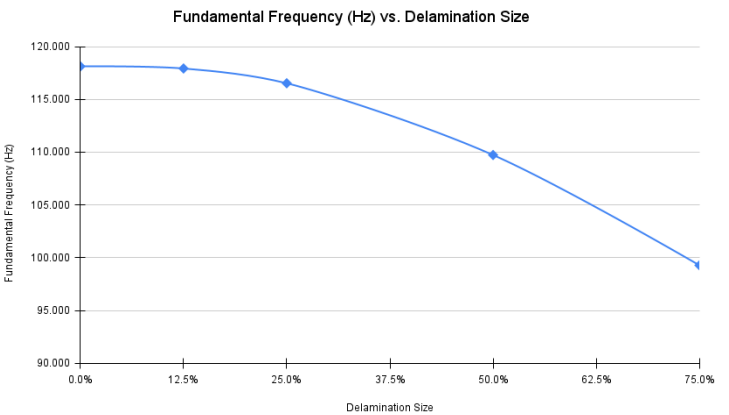

Figure 7: Graph of fundamental frequency against delamination size for $[0°]_8$ FFRE composite plate under SSSS boundary condition

Effect of delamination location

In order to analyse the variation of delamination location on the natural frequency of the $[0°]_8$ 25% delaminated FFRE composite plate, the delaminations were placed between the plies on the middle plane of the composite plate. Each delamination location was subjected to three different boundary conditions. The nine locations comprised the combination of normalised lengths of 0.35 l, 0.5 l, 0.65 l and normalised widths of 0.35 w, 0.5 w, and 0.65 w. Therefore, this section will discuss and analyse only the fundamental natural frequency.

CCCC boundary condition

The variation of fundamental natural frequency as a function of delamination location for CCCC condition was plotted in Figure 9. The figure shows that the maximum frequency is 219.996 Hz with centre delamination. Meanwhile, the minimum frequency is 201.098 Hz with delamination located at 0.35 l and 0.65 l of the middle of the width. Due to symmetry boundary conditions, the natural frequencies are mirrored with respect to the length-wise and width-wise vertical middle planes. Thus, the natural frequencies with delamination located at the corners are 205.622 Hz. For the first vibration mode, since the

boundary condition is four sides clamped, the natural frequencies for those delaminations positioned near the high shear force regions experienced stronger influence than those located at the high bending moment regions.

Table 7: Natural frequencies (Hz) for $[0°]_8$ FFRE composite plate under CFFF boundary condition with different delamination size

Mode	Delamination Size				
	0.0%	**12.5%**	**25.0%**	**50.0%**	**75.0%**
1	33.67	33.43	32.71	30.56	27.78
2	47.25	47.23	47.10	46.19	44.18
3	109.85	109.31	107.67	102.67	95.73
4	210.82	209.92	204.39	180.55	152.59
5	226.09	226.00	223.04	193.81	167.11
6	251.59	242.06	226.04	216.50	194.92
7	291.49	289.36	278.19	251.68	227.90
8	415.86	395.08	371.70	285.32	230.14
9	466.14	448.38	391.76	339.02	277.97
10	588.71	500.72	424.26	345.36	310.12

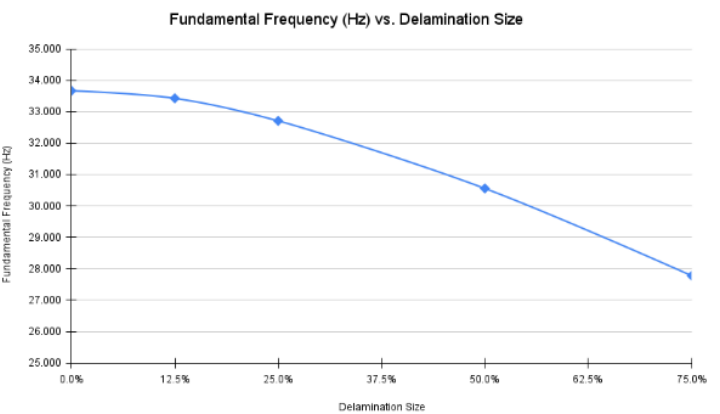

Figure 8: Graph of fundamental frequency against delamination size for $[0°]_8$ FFRE composite plate under CFFF boundary condition

Besides, it is also noticed that the natural frequencies for delamination located in the middle of the four edges do not have the same value. This is because the current study model's stacking sequence is $[0°]_8$. As a result, the elastic modulus in the length-wise direction is greater than the width-wise. Therefore, compared to the intact condition (235.62 Hz from Table 5), the natural frequencies decrease by 6.63%, 12.73%, 14.65% and 6.77% for

delamination positioned at the centre, corners, mid-span of widths edges and mid-span of length's edges respectively.

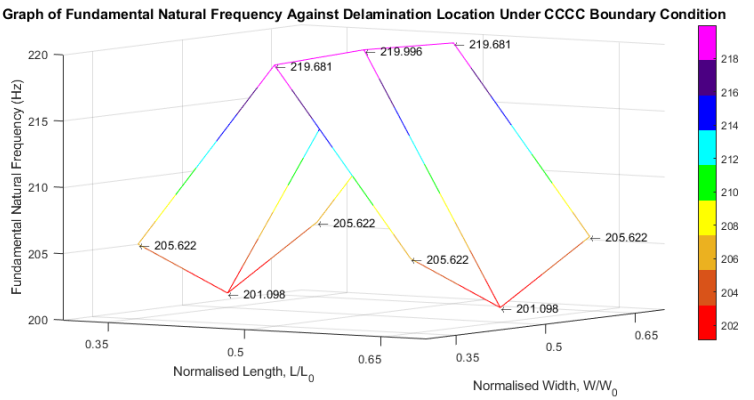

Figure 9: Graph of fundamental frequency against delamination location for $[0°]_8$ 25% delamination FFRE composite plate under CCCC boundary condition

SSSS boundary condition

Figure 10 shows the effects of delamination location on the fundamental natural frequency of the composite plate under SSSS conditions. As observed from the figure, the fundamental natural frequency as a function of delamination location for the SSSS condition has an identical trend to the CCCC condition, where the highest value occurred with centre delamination, which is similar to Zhang et al. [20]. The fundamental natural frequency of the SSSS supported composite plate with delamination located at the centre, corners, mid-span of width's edges, and mid-span of length's edges reduced by 1.35%, 3.61%, 3.96% and 1.76%, respectively, with respect to the natural frequency (118.12 *Hz* from Table 6) of the intact plate. The SSSS condition possesses a lower decrease in frequency due to the clamping effects of clamped edges producing greater elastic stiffness to the plate than the simply supported edges.

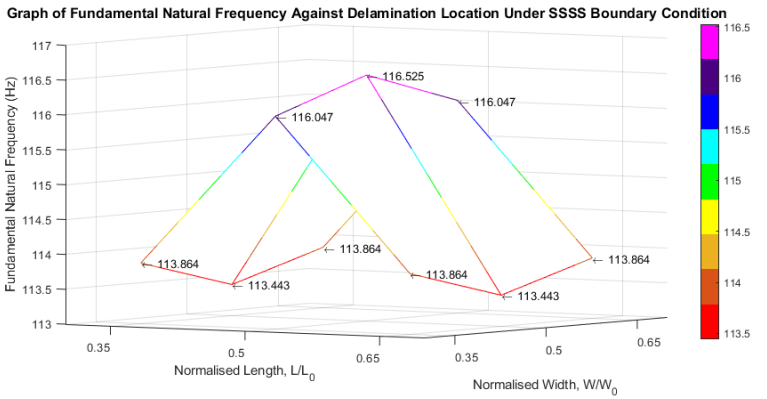

Figure 10: Graph of fundamental frequency against delamination location for $[0°]_8$ 25% delamination FFRE composite plate under SSSS boundary condition

CFFF boundary condition

The variation of delamination location on the fundamental natural frequency of the composite plate under CFFF condition was plotted in Figure 11. The trend presented by the CFFF condition is different from CCCC and SSSS conditions. Similar to the results of Goren Kiral et al. [6], the frequency increased with increasing normalised length. Therefore, the delamination located at the free end of the plate and near the length's edges possesses the greatest fundamental frequency (33.116 Hz). The lowest frequency delamination (32.557 Hz) is located near the mid-span, which is 0.35 l away from the clamped end.

The trend of this condition is different from the others because it is a cantilever plate. Thus, it has a higher shear force in the region close to the clamped end. Consequently, the natural frequency experiences greater reduction when the delamination is located near the clamped end, while the natural frequencies are close to the intact value for delamination positioned near the free end. Furthermore, the composite plate encounters greater frequency reduction for delamination located along the middle of the width. This is because the bending moment near the length's edges is greater than the middle region.

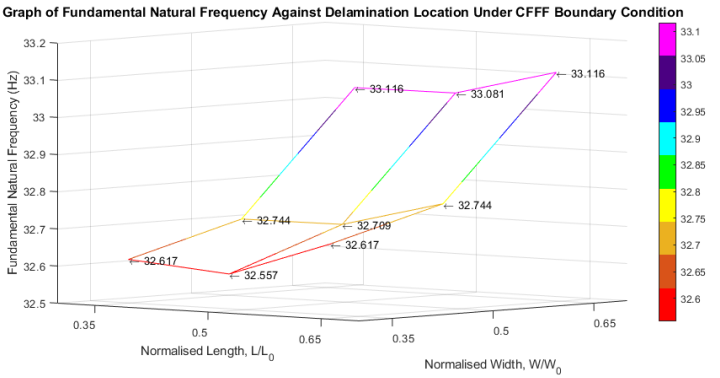

Figure 11: graph of fundamental frequency against delamination location for $[0°]_8$ 25% delamination FFRE composite plate under CCCC boundary condition

Conclusion

Based on the present results, the natural frequency of the delaminated composite plate is influenced by the clamping effects, with CCCC plate possess the greatest natural frequency. Besides, for increasing fibre orientation from 0° to 45°, the fundamental natural frequencies decrease for the CCCC condition and increase for the SSSS condition. On the other hand, the fundamental natural frequency for the CFFF condition decreases with increasing fibre orientation. Moreover, the increase of delamination size reduces the natural frequencies conspicuously for the three boundary conditions. Lastly, for CCCC and SSSS conditions, the centre delamination possesses the highest fundamental natural frequency. In contrast, the natural frequency increase with delamination is located near the CFFF condition's free end. The effect of delamination location on the natural frequency is greater along the length's direction than the width's direction. Understanding the vibration behaviour of delaminated natural fibre composite is beneficial to expand their usage in structural applications. The present study needs to be extended to compare the numerical results with experimental results.

Acknowledgement

This paper is done with the financial support from Tunku Abdul Rahman University College.

References

[1] D. Li, "Layerwise theories of laminated composite structures and their applications: a review," *Archives of Computational Methods in Engineering,* vol. 28, no. 2, pp. 577-600, 2021, https://doi.org/10.1007/s11831-019-09392-2.

[2] K. Torabi, M. Shariati-Nia, and M. Heidari-Rarani, "Experimental and theoretical investigation on transverse vibration of delaminated cross-ply composite beams," *International Journal of Mechanical Sciences,* vol. 115, pp. 1-11, 2016, https://doi.org/10.1016/j.ijmecsci.2016.05.023.

[3] N. Hu, H. Fukunaga, M. Kameyama, Y. Aramaki, and F. Chang, "Vibration analysis of delaminated composite beams and plates using a higher-order finite element," *International Journal of Mechanical Sciences,* vol. 44, no. 7, pp. 1479-1503, 2002, https://doi.org/10.1016/S0020-7403(02)00026-7.

[4] D. Shu and C. N. Della, "Vibrations of multiple delaminated beams," *Composite Structures,* vol. 64, no. 3-4, pp. 467-477, 2004, https://doi.org/10.1016/j.compstruct.2003.09.047.

[5] J. Mohanty, S. Sahu, and P. Parhi, "Numerical and experimental study on free vibration of delaminated woven fiber glass/epoxy composite plates," *International Journal of Structural Stability and Dynamics,* vol. 12, no. 02, pp. 377-394, 2012, http://dx.doi.org/10.1142/S0219455412500083.

[6] B. G. Kiral, Z. Kiral, and H. Ozturk, "Stability analysis of delaminated composite beams," *Composites Part B: Engineering,* vol. 79, pp. 406-418, 2015, https://doi.org/10.1016/j.compositesb.2015.05.008.

[7] M. Meon, N. M. Nor, S. Shawal, J. Saedon, M. Rao, and K.-U. Schröder, "On the Modelling Aspect of Low-Velocity Impact Composite Laminates," *Journal of Mechanical Engineering (JMechE),* vol. 17, no. 2, pp. 13-25, 2021, https://doi.org/10.21491/jmeche.v17i2.15297.

[8] D. X. Hung, T. M. Tu, and T. Dai Hao, "Free vibration analysis of laminated CNTRC plates using the pb2-Ritz method," *Journal of Mechanical Engineering (JMechE),* vol. 18, no. 1, pp. 213-232, 2021.

[9] H. Daoud, J.-L. Rebiere, A. Makni, M. Taktak, A. El Mahi, and M. Haddar, "Numerical and experimental characterization of the dynamic properties of flax fiber reinforced composites," *International Journal of Applied Mechanics,* vol. 8, no. 05, p. 1650068, 2016, http://dx.doi.org/10.1142/S175882511650068X.

[10] M. Rajesh and J. Pitchaimani, "Experimental investigation on buckling and free vibration behavior of woven natural fiber fabric composite under axial compression," *Composite Structures,* vol. 163, pp. 302-311, 2017, https://doi.org/10.1016/j.compstruct.2016.12.046.

[11] S. Mahmoudi, A. Kervoelen, G. Robin, L. Duigou, E. Daya, and J. Cadou, "Experimental and numerical investigation of the damping of

flax–epoxy composite plates," *Composite Structures*, vol. 208, pp. 426-433, 2019, https://doi.org/10.1016/j.compstruct.2018.10.030.

[12] V. Gopalan *et al.*, "Dynamic characteristics of woven flax/epoxy laminated composite plate," *Polymers*, vol. 13, no. 2, p. 209, 2021, http://dx.doi.org/10.3390/polym13020209.

[13] I. Tharazi *et al.*, "Effects of fiber content and processing parameters on tensile properties of unidirectional long kenaf fiber reinforced polylactic-acid composite," *Journal of Mechanical Engineering (JMechE)*, no. 1, pp. 65-76, 2017.

[14] S. Yunus, A. H. Abdullah, N. H. Abdul Halim, and Z. Salleh, "Low energy impact on the short kenaf fibre reinforced epoxy composites: Effect to the residual strength and modulus," *Journal of Mechanical Engineering (JMechE)*, vol. 12, no. 2, pp. 72-83, 2015.

[15] M. Ravandi, W. Teo, M. Yong, and T. Tay, "Prediction of Mode I interlaminar fracture toughness of stitched flax fiber composites," *Journal of Materials Science*, vol. 53, no. 6, pp. 4173-4188, 2018, https://doi.org/10.1007/s10853-017-1859-y

[16] Y. Shen, J. Tan, L. Fernandes, Z. Qu, and Y. Li, "Dynamic mechanical analysis on delaminated flax fiber reinforced composites," *Materials*, vol. 12, no. 16, p. 2559, 2019, https://doi.org/10.3390/ma12162559

[17] A. Harun, T. T. Sia, C. H. Che Haron, J. A Ghani, and S. Mokhtar, "A study on parameter optimization of the delamination factor (Fd) in Milling Kenaf fiber reinforced plastics composite materials using DOE method," *Journal of Mechanical Engineering (JMechE)*, no. 1, pp. 211-224, 2017.

[18] S. Ganesh, K. S. Kumar, and P. Mahato, "Free vibration analysis of delaminated composite plates using finite element method," *Procedia Engineering*, vol. 144, pp. 1067-1075, 2016, https://doi.org/10.1016/j.proeng.2016.05.061

[19] R. Samyal, S. Singh, and A. K. Bagha, "Modal analysis of composite panel at different fiber orientations," *Materials Today: Proceedings*, vol. 16, pp. 477-480, 2019, https://doi.org/10.1016/j.matpr.2019.05.118

[20] Z. Zhang, K. Shankar, M. Tahtali, and E. Morozov, "Vibration modelling of composite laminates with delamination damage," in *Proceedings of 20th International Congress on Acoustics, ICA*, 2010.